Available online at www.sciencedirect.com
ScienceDirect
Biochimica et Biophysica Acta 1778 (2008) 113 – 124
Biochimica et Biophysica Acta
BBA
www.elsevier.com/locate/bbamem

Interactions of the dipeptide paralysin β-Ala-Tyr and the aminoacid Glu with phospholipid bilayers

Ioanna Kyrikou [a], Nikolas P. Benetis [a,*], Petros Chatzigeorgiou [b], Maria Zervou [a], Kyriakos Viras [b], Constantine Poulos [c], Thomas Mavromoustakos [a,b,*]

[a] Institute of Organic and Pharmaceutical Chemistry, National Hellenic Research Foundation, Vas. Constantinou 48, Athens 11635, Greece
[b] National and Kapodistrian University of Athens, Department of Chemistry, Physical, Chemistry Laboratory, Panepistimioupolis Zographou, 157 71 Athens, Greece
[c] Department of Chemistry, University of Patras, GR-26500, Patras, Greece

Received 16 May 2007; received in revised form 31 August 2007; accepted 12 September 2007
Available online 2 October 2007

Abstract

Existing evidence points out that the biological activity of β-Ala-Tyr may in part related to its interactions with the cell membranes. For comparative reasons the effects of Glu were also examined using identical techniques and conditions. In order to examine their thermal and dynamic effects on membrane bilayers a combination of DSC, Raman and solid state NMR spectroscopy on DPPC/water model membranes were applied and the results were compared. DSC data showed that Glu perturbs to a greater degree the model membrane compared to β-Ala-Tyr. Thus, alteration of the phase transition temperature and half width of the peaks, abolishment of the pretransition and influence on the enthalpy of the phase transition were more pronounced in the Glu loaded bilayers. Raman spectroscopy showed that incorporation of Glu in DPPC/water bilayers increased the order in the bilayers in contrast to the effect of the dipeptide. Several structural and dynamical properties of the DPPC multilamellar bilayers with and without the dipeptide or Glu were compared using high resolution C-13 MAS (Magic Angle Spinning) spectra and spectral simulations of inhomogeneously broadened, stationary P-31 NMR lineshapes measured under CP (Cross-polarization) conditions. These methods revealed that the aminoacid Glu binds in the close realm of the phosphate in the hydrophilic headgroup of DPPC while β-Ala-Tyr is located more deeply inside the hydrophobic zone of the bilayer. The P-31 NMR simulations indicated restricted fast rotary motion of the phospholipids about their long axes in the organized bilayer structure. Finally, by the applied methodologies it is concluded that the two molecules under study exert dissimilar thermal and dynamic effects on lipid bilayers, the Glu improving significantly the packing of the lipids in contrast to the smaller and opposite effect of the dipeptide.

Keywords: Paralysin β-Ala-Tyr; C-13 MAS NMR; CP P-31 NMR broadline, differential scanning calorimetry DSC; DPPC/water bilayer; Raman spectroscopy; The aminoacid neurotransmitter Glutamate (L-Glu)

1. Introduction

β-Ala-Tyr (Fig. 1) is a toxin obtained from the larvae of the gray flesh fly Neobelleria bullata, which is synthesized in the fat body and is known to accumulate in the larval haemolymph up to the moment of the formation of the white puparium [1].

Intraspinal injections in rats with β-Ala-Tyr, result in prolonged hindleg paralysis with severe histologically visible neural lesions, whereas similar injections in rats with saline have no toxic effect [2].

The aminoacid Glutamate (L-Glu) is the neurotransmitter at most fast excitatory synapses in the mammalian central nervous system (CNS). It plays an important role in synaptic plasticity phenomena involved in brain development such as LTP (Long Term Potentiation) and LTD (Long Term Depression), learning and memory. Glutamate is also the main endogenous neurotoxin, being responsible for neuronal death observed after ischemy, hypoxy or hypoglycemy and is therefore assumed to

* Corresponding authors. Institute of Organic and Pharmaceutical Chemistry, National Hellenic Research Foundation, Vas. Constantinou 48, Athens 11635, Greece. Fax: +30107273831.
E-mail addresses: niben@eie.gr (N.P. Benetis), tmavro@eie.gr (T. Mavromoustakos).

0005-2736/$ - see front matter © 2007 Elsevier B.V. All rights reserved.
doi:10.1016/j.bbamem.2007.09.019

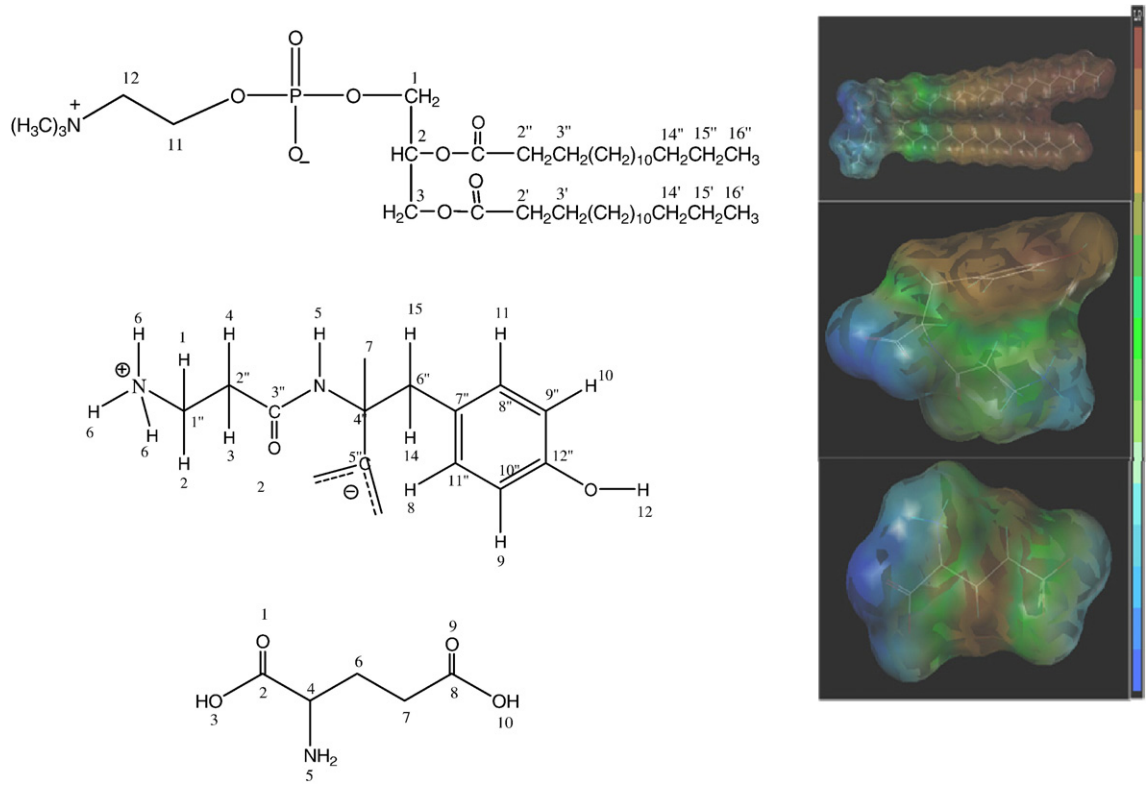

Fig. 1. Molecular structures and lipophilic profiles of the phospholipid (D-Palmitoyl-glycero-sn-3-Phosphatidyl-Choline) DPPC, the dipeptide beta-alanine-tyrosine (β-Ala-Tyr) and the aminoacid glutamate (L-Glu). Notice the significantly larger lipophilic potion of the dipeptide due to the benzyl ring in contrast to the faintly exposed to the solvent lipophilic part of Glu.

be involved in some neurological disorders such as Parkinson's and Alzheimer's diseases. L-Glutamate is acting through both ligand-gated ionic channels (ionotropic) and G-protein coupled (metabotropic) receptors [3].

The ionotropic receptors are multimeric glutamate-gated channels permeable to cations and responsible for fast depolarization. Three subtypes have been characterized based on their channel properties, pharmacology, and subunit composition. They are termed NMDA (*N*-methyl-D-aspartate), AMPA (α-amino-3-hydroxy-5-methylisoxazole-4-propionate) and KA (kainate) receptors. The metabotropic glutamate receptors (mGluRs) which have been characterized more recently are G-protein coupled receptors (GPCRs) and modulate the activity of ionic channels or enzymes by producing second messengers.

Today, eight mGluRs have been characterized and classified into three groups based on their sequence, homology, transduction mechanism and pharmacology [4,5]. mGluRs belong to a distinct family of GPCRs, which includes $GABA_B$ receptors, Ca^{2+} sensing receptors and others. Among the main distinguishing features of this class of receptors is a large N-terminal ligand binding domain and the distinct location of G-protein coupling domains.

We sought to study the interactions of β-Ala-Tyr and its topology in the membranes mainly because of two reasons. First, the binding site for Glu is known in contrast to β-Ala-Tyr. Therefore, by studying their effects on lipid bilayers we could also infer on their effects on the receptor site. Second, β-Ala-Tyr has antimicrobial action to both $Gram^+$ and $Gram^-$ bacteria [6]; hence, it is interesting to know whether the differences of the antimicrobial action between β-Ala-Tyr and Glu are related to the membrane bilayer interaction. The L-α-DPPC model-membrane bilayers in water were chosen for the present study since (a) the mesomorphism of DPPC/water bilayers is well studied using various biophysical methods, and (b) other drugs were studied in our laboratory using the same phospholipid [7] in an attempt to explore their thermal effects and relate these with their stereo-electronic features.

The difficulties due to the inhomogeneous broadening in solid-state NMR spectroscopy can be avoided by using the MAS (Magic Angle Spinning) technique. This method was utilized in the present work in order to obtain high-resolution ^{13}C-spectra of the partially immobilized lamellar formations of the DPPC-water dispersions, without and with the toxin or the Glu molecules incorporated. The temperature-dependent variation of the isotropic chemical shifts, the intensities and the half-widths of the NMR peaks, as well as the different T_1s of the carbon atoms of the phospholipid have been used in the qualitative determination of the mobility of the different parts of the lipid molecules. These properties were interpreted as measures of the toxin or Glu interaction with the bilayers.

In addition to the ^{13}C-MAS spectra, simulations of the powder ^{31}P-NMR spectra obtained without MAS of the samples were performed.

The simulations of powder ^{31}P-NMR spectra of stationary samples were based on the residual anisotropy of the CSA (Chemical Shift Anisotropy) or shielding tensor [8] of the ^{31}P

nucleus because of the restricted motion of the phospholipids imposed by the immobilized bilayers [9]. By the simplified dynamics model of the present work it is assumed that internal motions of the phosphate in the lipid molecules do not contribute significantly to the statistical averaging of the magnetic interactions. On the other hand, by attributing the motion of the hydrophilic head-group region to the overall rotation of the lipids a reasonably good account of the configuration and of the dynamics in the entire DPPC bilayers was possible.

Application of a standard pulse sequence involving CP (Cross Polarization) and acquisition of the signal under proton decoupling resulted in signal enhancement by the Dipole–Dipole (DD) Phosphorous–Proton interaction [10]. A structural and dynamical model exploring the anisotropy of the above two magnetic interactions (CSA and DD) was utilized for the simulation of the ^{31}P NMR powder lineshapes in order to extract information about the hydrophilic environment of the head-group region in the DPPC multibilayers.

Appreciable NMR work has been devoted to ^{31}P lineshapes of membrane bilayers and natural membranes. In the particularly useful review by Yeagle [11] as well in the earlier work by Frye et al. [12] some of the characteristics of the powder lineshapes seen also in the present work for the non-MAS CP ^{31}P case were explained qualitatively. A quantitative theory of the ^{31}P broadlines for slow-motion dynamics of the P-31 chemical shift anisotropy has been published earlier [13]. In the present work the recently developed by our group P-31 broadline simulation program for the limiting case of slow overall bilayer motion under fast overall rotation of the lipids is applied on new experimental data. The theoretical background of this work was established earlier [9].

In addition to NMR, Raman Spectroscopy revealing the *trans-gauche* transformations of the alkyl chain for thermal and conformation variation, as well as DSC for the investigation of the thermotropic changes of the bilayers were applied.

2. Materials and methods

2.1. Materials

Dipalmitoyl-glycero-*sn*-3-phosphorylcholine (DPPC) was obtained from Avanti Polar Lipids Inc., AL, USA. β-Ala-Tyr was synthesized in the Laboratory of Organic Chemistry, Department of Chemistry, University of Patras. Spectroscopic grade $CHCl_3$ (+99%) was purchased from Sigma-Aldrich (O.M.) Ltd. Athens, Greece. Stainless steel capsules were obtained from Perkin-Elmer MA, USA. The dipeptide β-Ala-Tyr and the Glu used in this research work had a minimum purity of 99% (TLC).

2.2. Methods

2.2.1. Sample preparation

For the DSC, Raman and solid-state NMR experiments identical procedures were followed for the liposome preparation. For each sample, appropriate amounts of DPPC with or without the dipeptide or Glu were dissolved in spectroscopic grade chloroform.

After mixing, the solvent was evaporated by passing a stream of N_2 over the solution at 50 °C and the residue was placed under vacuum (0.1 mm Hg) for 24 h. For measurements, this dry residue was dispersed in appropriate amounts of bidistilled water by vortexing.

2.2.2. Differential Scanning Calorimetry DSC

After dispersion in water (50% w/w), portions of the samples (ca. 5 mg) were sealed in stainless steel capsules obtained from Perkin-Elmer. Thermograms were obtained in a Perkin-Elmer DSC-7 calorimeter. Prior to scanning, the samples were held below their phase transition temperature for 1–2 min to ensure equilibration. All samples were scanned at least twice until identical thermograms were obtained, using a scanning rate of 2.5 °C/min. The temperature scale of the calorimeter was calibrated using indium (T_m = 156.6 °C) and DPPC bilayers (T_m = 41.2 °C).

2.2.3. Solid-State NMR spectroscopy

High-resolution NMR ^{13}C-spectra were obtained at 100.63 MHz on a Bruker MSL 400 NMR spectrometer capable of high-power ^{1}H-decoupling and equipped with MAS (Magic Angle Spinning) unit. The decoupling strength used was 50 W (13H).

For MAS spectra, a 4 mm rotor, 2.5 kHz rate and 100 Hz line broadening were used. The spinning rate for MAS NMR experiments was kept constant for all the temperatures 25–45 °C.

The temperatures of this range cover all mesomorphic states of DPPC/water bilayers samples in the present work. Each spectrum was an accumulation of 1000 scans. The lipid content for the two samples used in the experiments was the same (~40 mg). The delay time used was 6 s, the 90° pulse width was 5 μs and the acquisition time was 40 ms. Chemical shift values of DPPC bilayers were obtained from literature [14]. Peak assignments attributed to β-Ala-Tyr (see Table 2) and Glu are based on their ^{13}C high resolution (HR-NMR) data in solution [15].

The acquisition of the static ^{31}P-NMR spectra was performed for central ^{31}P frequency 161.277 MHz in the temperature range 25–49 °C. They were obtained using a standard cross polarization technique from the BRUKER libraries and high power decoupling with the rotor positioned in a magic angle relative to the magnetic field. The particular pulse sequence enables Cross Polarization of the ^{31}P nucleus by spin locking of the protons which then obtain the Hartman–Hahn condition with respect to the ^{31}P frequency in their own rotating frame. The recycle delay used was 4 s, the 90° pulse 5.0 ms and the contact time for CP experiments was 1 ms, as it gave the optimal signal. Each spectrum was typically an accumulation of 4000 scans.

2.2.4. Raman spectroscopy

The Raman spectra were obtained at 4 cm^{-1} resolution from 3500 to 400 cm^{-1} with interval 2 cm^{-1} using a Perkin-Elmer NIR FT-spectrometer (Spectrum GX II) equipped with CCD detector. The measurements were performed at a temperature range of 25°–43 °C. The laser power and spot (a Nd: YAG at 1064 nm) were controlled to be constant at 400 mW during the experiments. 1500 scans were accumulated and back scattering light was collected.

3. Results and discussion

3.1. Differential Scanning Calorimetry

Hydrated DPPC lipids spontaneously form multi-lamellar bilayers whose dynamic and thermotropic properties have been extensively studied by various biophysical methods such as e.g. DSC and solid state NMR [16].

The DPPC molecules form at the lower temperatures a well organized lamellar gel phase, L'_β, while at high temperatures they obtain the liquid crystalline phase, L_a, which has greater fluidity. An intermediate phase, P'_β, is also observed, at which the bilayers are distorted by a periodic ripple [16] (ripple phase) [17]. The DPPC bilayers exist in the gel phase for temperatures lower than 35.3 °C and in the liquid crystalline for temperatures above 41.2 °C (Table 1). The thermal changes caused by the inclusion of the dipeptide or Glu in the DPPC bilayers are shown in Fig. 2.

The most prominent feature during phase transitions is the *trans-gauche* isomerisation taking place in the alkyl chain conformation [18]. Increased average number of *gauche* conformers indicates greater effective fluidity, which depends not only on the temperature, but also on perturbations due to the presence of a drug molecule intercalating between the lipids.

The obtained DSC scans of the fully hydrated DPPC/water multibilayers showed a *pretransition* centered at 35.3 °C and a *main transition* at 41.2 °C. The addition of a small amount of β-Ala-Tyr to a 1% molar ratio (β-Ala-Tyr/DPPC, $x=0.01$) caused only minor effects in the pre-transition and main phase transition. At higher molar ratios β-Ala-Tyr/DPPC ($x=0.05$ and $x=0.10$) the pretransition was broadened and the temperature of the main phase transition was slightly lowered. The decreasing temperature of the phase-transition feature indicated that the alkyl chain region became more fluid. This can be understood by the localization of the dipeptide in the higher region of the hydrophobic region close to the glycerol backbone, as the other methods of the present work verify. At the highest experimental molar ratio in this series ($x=0.20$) the dipeptide abolished the pretransition and broadened the main phase transition. The quantitative results of these experiments are presented in Table 1 where the variation of T_m, $T_{m;1/2}$ and ΔH versus molar concentration of β-Ala-Tyr or the Glu is compared with the unloaded DPPC/water bilayers. T_m was constant at concentrations of β-Ala-Tyr up to $x=0.10$ and decreased at the highest concentration of $x=0.20$. $T_{m;1/2}$ was increased as the concentration increased and decreased at $x=0.20$. ΔH was almost concentration independent.

On the other hand, Glu caused stronger perturbing effects than β-Ala-Tyr. Already at the lowest experimental concentrations of molar ratios Glu/DPPC $x=0.01$ and $x=0.05$ Glu induced an enhanced broadening of the main phase transition and abolished the pretransition. This behaviour indicated that the aminoacid interacted strongly with the phosphate headgroup [19]. Interestingly, the main phase transition temperature T_m is increased showing a strong association in the membrane bilayers due to the presence of the aminoacid. At higher concentration (i.e. $x=0.10$) a shoulder appeared at the lower right wing of the phase-transition thermogram, probably showing some inhomogeneity in the bilayers. At molar concentration $x=0.20$ the shoulder is more prominent. The most reasonable explanation corroborating with NMR experimental results is that various domains are formed. At 40 °C the broad transition of small intensity probably indicated pure DPPC bilayers. The main peak and shoulder indicated the existence of DPPC bilayers containing different concentrations of Glu. At high concentrations of $x=0.10$ and $x=0.20$, while the inhomogeneity is increased the breadth of the phase transition is decreased. T_m and ΔH decreased with increasing molar concentration of Glu while $T_{m;1/2}$ showed an opposite effect. These features are seen in Table 1.

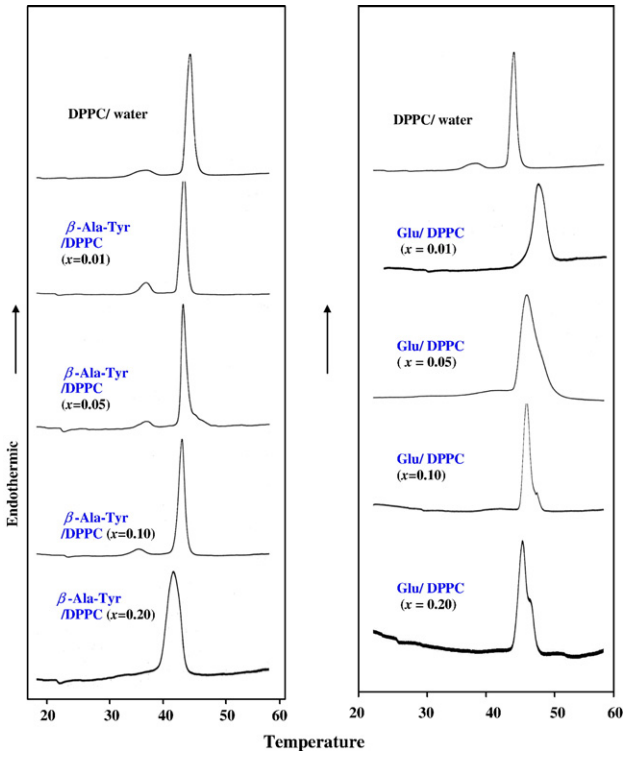

Fig. 2. Normalized DSC scans of fully hydrated DPPC/water bilayers with and without β-Ala-Tyr or L-Glu.

Table 1
Values of onset (T_{onset}) and phase-transition temperatures T_m for the main transition, half width of the main transition peak $T_{m;1/2}$ and enthalpy changes (ΔH) of the studied preparations

Sample (molar ratio x)	T_{onset} (°C)	SD	$T_{m'}$ (°C)	SD	$T_{m;1/2}$	SD	ΔH (J/g)	SD
DPPC	39.56	0.09	41.20	0.06	0.20	0.02	45.52	0.23
β-Ala-Tyr/ DPPC ($x=0.01$)	39.19	0.01	40.35	0.02	0.18	0.02	45.34	0.13
β-Ala-Tyr/ DPPC ($x=0.05$)	38.15	0.03	40.22	0.04	0.15	0.03	44.98	0.03
β-Ala-Tyr/ DPPC ($x=0.10$)	37.84	0.07	40.16	0.04	0.18	0.01	44.52	0.08
β-Ala-Tyr/ DPPC ($x=0.20$)	36.60	0.06	38.97	0.02	0.40	0.02	43.69	0.03
Glu/DPPC ($x=0.01$)	44.56	0.04	45.96	0.02	0.40	0.02	38.83	0.11
Glu/DPPC ($x=0.05$)	43.84	0.03	45.78	0.06	0.50	0.03	37.39	0.04
Glu/DPPC ($x=0.10$)	42.65	0.05	44.56	0.04	0.20	0.03	32.20	0.05
Glu/DPPC ($x=0.20$)	42.47	0.02	43.95	0.04	0.30	0.01	22.43	0.15

Also the standard deviations SD of the measurements calculated from three repetitions are given.

3.2. NMR spectroscopy

3.2.1. High Resolution ^{13}C MAS spectra

To gain direct evidence on the incorporation of the dipeptide and Glu in DPPC bilayers representative solid state ^{13}C/MAS-NMR spectra for the preparations under study [18]. The spectra were divided into two regions. The first comprised carbon atoms in the hydrophobic region (10–40 ppm) and those in the glycerol backbone and head group region (40–80 ppm) (Fig. 3). The second region above 110 ppm (downfield) comprised the aromatic carbons and the esterified carbonyls, which appeared near 170 ppm (Fig. 4).

When the two bioactive molecules of the present study were incorporated into phospholipid bilayers caused the following modifications to the ^{13}C-NMR spectrum. (a) Changed the peak intensity and line-width due to the modified bilayer fluidity; (b) changed the chemical shift values of the individual carbon nuclei of the bilayer lipids; (c) brought about a specific subset of additional peaks attributed to carbon nuclei of the incorporated molecule.

Below the phase transition temperature (gel phase) the carbonyl signal was broad and asymmetric. Above the phase transition (liquid crystalline phase) where the fluidity of the membrane was increased, this peak became narrower. Other peaks also above the phase transition temperature became narrower and additional peaks were resolved. Above the main phase transition temperature several changes were observed not only in the lineshape of the peaks but also in their chemical shifts. For examples, an upfield shift of the $(CH_2)_n$ peaks was observed which reflected an increase in the acyl chains population of gauche conformations [18].

The preparations containing the dipeptide showed additional peaks (labelled on the top of the peaks in Figs. 3, 4) due to its presence in the lipid bilayers. The assignments of the peaks were achieved using high-resolution 1D and 2D experiments (HSQC, HMBC, see Table 2). These additional peaks originated from the polar and non-polar regions of the dipeptide. Glu peaks appeared also in the esterified carbonyl region and the polar headgroup. The results indicated that both molecules were incorporated in the bilayer core.

The broad featureless peak at 30 ppm was attributed to $(CH_2)_{10}$ of DPPC alkyl chains and was the most diagnostic of the mesomorphic changes which occurred in DPPC bilayers as the temperature increased. Its upfield shift and narrowing depicted the phase transition of the phospholipid bilayers from the gel phase or solid state to the liquid crystalline phase. During the phase transition trans-gauche isomerization of the alkyl chains occurred. The presence of *β*-Ala-Tyr or Glu caused increase of the breadth of the $(CH_2)10$ peak and an increase of the intensity in the terminal methyl group peak. The most pronounced effect was caused by the presence of Glu. The increase of the breadth was in harmony with DSC data which showed that for molar ratio Glu/DPPC $x=0.20$ drug concentration the width of the phase transition was increased due to the formation of domains or increase of sample inhomogeneity.

During the phase transition, the lineshape of the peak assigned to the esterified carbonyl groups changed. The broad, low intense peak at gel phase narrowed and increased in intensity in the liquid crystalline phase. The sharpening of the peak was evident in DPPC bilayers at 45 °C, a temperature above the phase transition.

The hydrophilic headgroup was not affected by the presence of *β*-Ala-Tyr but clearly the carbonyl region was more fluid or disordered (Fig. 4). The presence of Glu in DPPC bilayers resulted in upfield shift both in the gel and liquid crystalline phase.

The ^{13}C T_1 data in Fig. 5 indicated that the mobility of the headgroup was generally smaller than the mobility of the lipophilic area where there exist additional motional degrees of freedom. This is supporting our overall rotation model as a principal cause of the particular restricted-motion lineshape. In the case that intramolecular rotation of the phosphate dominated the axial averaging one should expect greater mobility of the headgroup. The above conclusions are however invalid if different relaxation mechanisms are active in the acyl chain or if the dipolar interaction with the protons in the head group is larger. Given the complexity of the system an alternative explanation is thus possible. That is, in spite of expected greater mobility of the headgroup, its modes of motion could exceed significantly the Larmor frequency of the C-13 at ca 100 MHz rendering the relevant relaxation mechanism of the headgroup carbons inefficient.

Furthermore the T_1 data in Fig. 5 demonstrated that either the dipeptide or the Glu molecules increased the flexibility of the $(-CH_2-)_{10}$ and the $-N^+(CH_3)_3$ regions of the lipid bilayers in both the gel and liquid crystalline phases. It was however noteworthy that the temperature dependence of T_1 in the DPPC/water/Glu sample was inverted for the lipophilic area of the

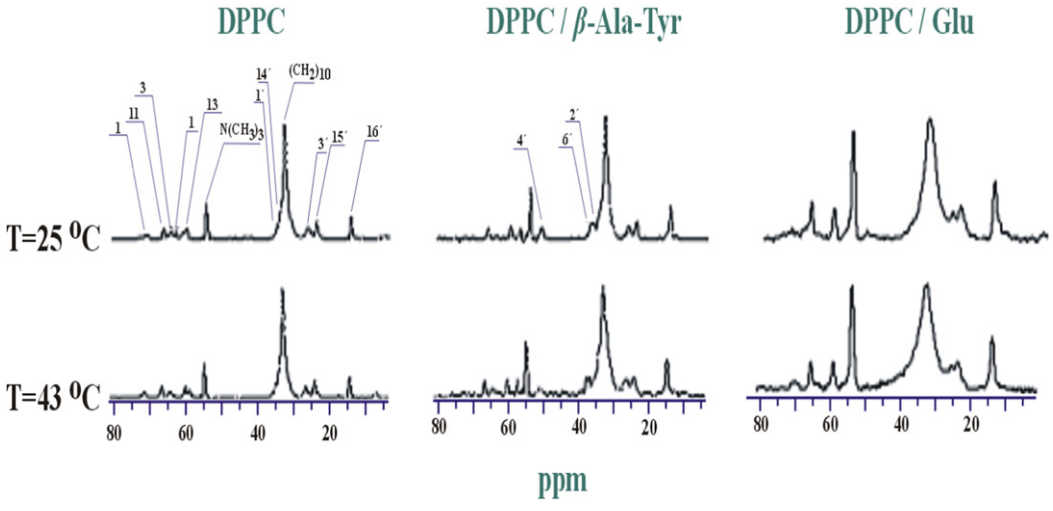

Fig. 3. The region between 0 and 80 ppm of ^{13}C-MAS (Magic Angle Spinning) spectra of DPPC/water bilayers for the two temperatures 25 and 43 °C. Left: Unloaded DPPC/water bilayers. Middle: DPPC/water/*β*-Ala-Tyr ($x=0.20$). Right: DPPC/water/Glu ($x=0.20$).

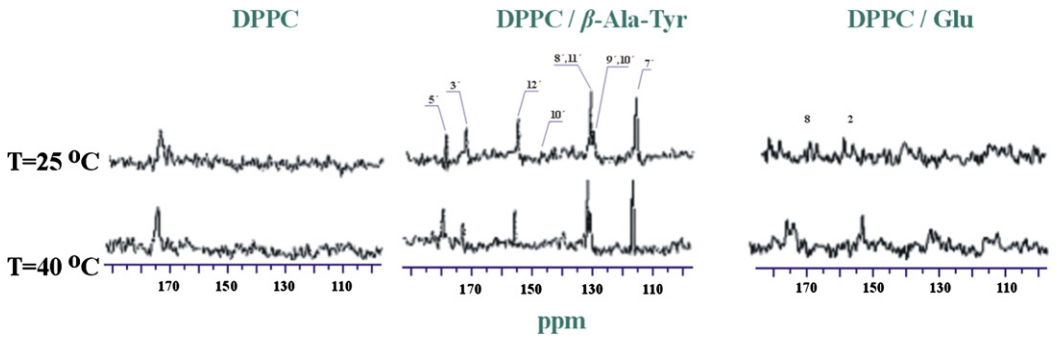

Fig. 4. Representative temperature variation of ^{13}C-MAS NMR spectra for DPPC/water bilayers, bilayers loaded with β-Ala-Tyr (x=0.20) and with Glu (x=0.20) in the region between 100 and 180 ppm.

bilayers. This fact, can be explained by assuming that the Glu decreases the mobility of the lipids, in agreement with the P-31 broadlines simulations to follow, and brings the relaxation conditions of the lipid molecules into the spin diffusion limit [20]. This is equivalent to the slow-motion regime of the Redfield conditions [21], and was already pointed out in our earlier work [9].

In order to obtain additional information about the topology of the two molecules in the membrane bilayers and about the dynamics of the system in absence and presence of the inclusion of the β-Ala-Tyr or the Glu broadline CP ^{31}P-NMR spectroscopy using static samples was applied.

3.2.2. Static CP (Cross Polarization) ^{31}P-NMR spectral simulations

The experimental ^{31}P-NMR lineshapes of the three multibilayer DPPC/water preparations with the absence or presence of the dipeptide β-Ala-Tyr or the aminoacid Glu were compared in order to obtain information about the dynamic effects of the dipeptide and the aminoacid. For temperatures lower than 240 K the phospholipid macromolecules are totally immobilized leading to a rhombic environment about the ^{31}P-nucleus as it has been determined from the characteristic inhomogeneously broadened lineshape due to the residual anisotropy of the Zeeman interaction [22]. The current experimental, static CP broadlines displayed axial symmetry. The axial symmetry of the spectra at the ambient temperatures and up to 50 °C indicated uniaxial rotation of the headgroup of the lipid molecules. They were also characterized by a sizable minimum located closer to the perpendicular edge of the powder lineshape. The position of the minimum corresponded to the isotropic average of the CSA (Chemical Shift Anisotropy) tensor or equivalently to its MA (Magic Angle) orientation with respect to the magnetic field. The experimental variable CP (Cross Polarization) efficiency in the different regions of the inhomogeneously broadened ^{31}P-NMR powder spectrum depended on the inclusion (dipeptide or Glu) and changed with the temperature. The characteristic minimum was more prominent for the higher measurement temperatures at which the bilayers are in the *liquid-crystalline* phase.

A minimal dynamical model was required in order to account for the experimental broadline CP ^{31}P-NMR spectra obtained for static samples in the temperature interval 25–49 °C. Details of this model were published elsewhere [9]. Interpreting the broadline spectral simulations we noted: (a) the inhomogeneous broadening indicated immobilized lamellar structures; (b) the axial lineshape required an apparently cylindrical CSA tensor indicating that a fast restricted rotary motion prevailed about the phosphate; (c) the position of the minimal CP efficiently indicated an effectively axial DD (Dipole–Dipole) tensor coinciding with the CSA tensor; (d) the direction of the overall rotation axis of the lipids was not necessarily perpendicular to the lamellae,

Table 2
^{13}C-NMR chemical shifts in DMSO, D_2O and DPPC bilayers for β-Ala-Tyr

Assignment	Chemical shifts		Chemical shifts
	DMSO	D_2O (literature)	DPPC bilayers (25 °C)
C-1′	33.64	31.7	[a]
C-2′	36.46	35.6	36.37
C-3′	169.97	171.9	170.01
C-4′	56.90	54.5	57.36
C-5′	225.25	–	–
C-6′	36.69	36.0	37.22
C-7′	129.72	128.6	130.16
C-8′, C-11′	129.89	130.6	131.13
C9′, C-10′	114.84	115.5	116.08
C-12′	155.54	154.5	154.91

[a] Overlapped with DPPC $(CH_2)_{10}$ peak.

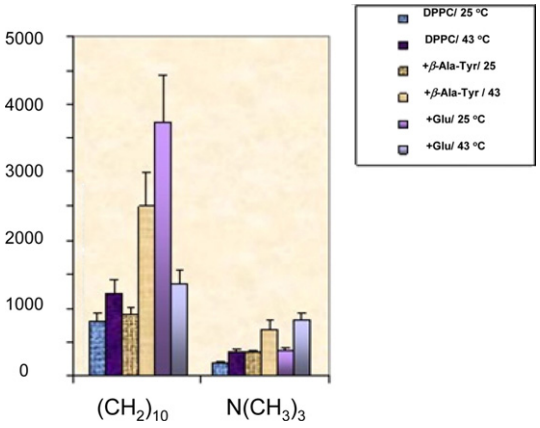

Fig. 5. C-13 T_1 values for $(-CH_2-)_{10}$ and the $-N^+(CH_3)_3$ groups in the absence and presence of either β-Ala-Tyr or Glu. The scale of the vertical axis is in ms.

indicating a collective tilt of the long axis of the lipid macromolecules in the bilayer leaflets. (Restricted uniaxial rotation of a minor fragment of the headgroup containing the phosphate is considered to be of minor influence in the present model.)

A summary of the obtained structural and magnetic parameters from the lineshape simulations is given in Table 3, which were further used to construct temperature profiles for the three most important simulation parameters out of totally six used in this study. The system is complicated and certainly needs more than six parameters to be described in detail therefore further development of the model is in process. However, this minimal model gives so far reasonable results about the most important dynamic properties of the present system.

The initial values of the (Chemical Shift Anisotropy) CSA-tensor components used for the simulations were, (−81, −21, 108) *ppm,* [22,9] while the variation seen in Table 3 to fit the experimental spectra conserved the anisotropy of the CSA-tensor. Thus the absolute value of the σ^{iso} in the present study has not any significance. However, the isotropic shift of the unloaded DPPC/water bilayers was comparable to the values of the loaded preparations and revealed greater proximity of the Glu to the phosphate in comparison to the dipeptide.

The simulations of the DPPC bilayers sample including Glu depicted in Fig. 6 differed significantly in several aspects both from the pure DPPC/water bilayers and the DPPC/water/β-Ala-Tyr bilayers sample. The lipid bilayers were much more affected by the presence of the Glu inclusion according to the quantitative results (simulation parameters) in Table 3;

(a) The presence of Glu in the DPPC bilayers gave a significant downfield shift in contrast to the dipeptide which caused a small opposite (upfield) shift.
(b) The angle between the Director and the Rotation axis ϑ_{DR} (collective tilt) was significantly larger in the DPPC bilayers containing Glu reaching angles a little over 45 degrees and showed relatively small variation of the CP-enhancement.

Table 3
Temperature dependence of the simulation parameters of static P-31 CP NMR lineshapes in (a) Unloaded DPPC/water bilayers, (b) DPPC/water bilayers containing inclusion of β-Ala-Tyr, or (c) Glu

Confidence/shape [a]	Temp/K/°C	brd/ppm	CSA tensor/ppm	(α, β)	$\Delta\sigma^{aniso}$/ppm	σ^{iso}/ppm	eNOE	ϑ_{DR}	V_0/K
(a) DPPC/water									
0.01/G	298/30	12.81	(−68.60, −8.60, 120.6)	(20.0, 33.74)	74.90	14.47	0.244	21.72	6.06E-03
0.01/G	303/30	11.81	(−69.29, −9.29, 119.91)	(20.0, 34.04)	73.55	13.77	0.276	20.6	9.36E-03
0.01/G	306/33	11.17	(−69.75, −9.75, 119.4)	(20.0, 34.58)	71.10	13.29	0.303	16.48	5.20E-03
0.01/L	309/36	6.49	(−69.68, −9.68, 119.4)	(20.0, 36.28)	63.46	13.35	0.607	9.01	4.53E-03
0.005/L	311/38	6.20	(−70.25, −10.25, 118.8)	(20.0, 36.23)	63.67	12.75	0.608	8.57	1.41E-03
0.01/L	313/40	4.11	(−68.18, −8.18, 120.8)	(20.0, 37.09)	59.72	14.82	0.749	5.53	3.50E-03
0.01/L	316/43	6.10	(−67.66, −7.66, 121.34)	(20.0, 37.31)	58.72	15.34	0.755	7.37	1.68E-03
0.005/L	319/46	2.62	(−67.71, −7.71, 121.3)	(20.0, 38.68)	52.39	15.29	0.882	4.77	5.00E-03
0.005/L	322/49	2.41	(−67.69, −7.69, 121.3)	(20.0, 38.58)	52.86	15.31	0.855	5.6	4.63E-03
(b) DPPC/water/β-Ala-Tyr									
0.01/G	298/25	12.78	(−74.50, −14.50, 114.5)	(20.0, 33.69)	75.02	8.50	0.295	13.25	5.51E-03
0.01/G	303/30	13.33	(−69.60, −9.60, 119.3)	(20.0, 34.00)	73.61	13.37	0.473	13.27	3.29E-03
0.01/G	306/33	10.31	(−69.42, −9.42, 119.5)	(20.0, 34.45)	71.63	13.24	0.351	9.51	7.77E-03
0.01/G	309/36	9.40	(−69.76, −9.76, 119.2)	(20.0, 34.92)	69.55	13.24	0.353	5.78	6.79E-03
0.005/L	311/38	6.26	(−70.12, −10.12, 118.9)	(20.0, 35.83)	65.45	12.88	0.408	5.16	7.38E-03
0.01/L	313/40	5.84	(−68.15, −8.15, 119.7)	(20.0, 36.36)	63.07	13.62	0.460	4.57	3.67E-03
0.01/L	316/43	4.61	(−69.40, −9.40 120.9)	(20.0, 37.14)	59.49	14.86	0.610	4.30	3.15E-03
0.005/L	319/46	3.99	(−67.45, −7.45, 121.6)	(20.0, 38.3)	53.93	15.56	0.771	2.41	2.55E-03
0.005/L	322/49	2.85	(−69.78, −9.78, 119.2)	(20.0, 39.37)	49.16	13.23	0.861	3.04	5.83E-03
(c) DPPC/water/Glu									
0.0075/G	298/25	18.59	(−62.96 −2.96 126.0)	(20.0, 31.08)	86.20	20.02	0.422	54.42	2.97E-03
0.0085/G	303/30	13.36	(−69.76, −9.76, 119.2)	(20.0, 34.70)	70.48	13.21	0.540	52.87	7.17E-03
0.0085/G	306/33	14.31	(−63.67, −3.67, 125.3)	(20.0, 33.88)	70.51	13.22	0.738	51.84	6.22E-03
0.01/L	309/36	11.50	(−64.91, −4.91, 124.0)	(20.0, 36.97)	60.25	18.06	0.794	44.85	4.98E-03
0.01/L	311/38	11.56	(−65.88, −5.88, 123.1)	(20.0, 36.76)	61.22	17.12	0.837	46.53	5.74E-03
0.005/L	313/40	10.99	(−66.04, −6.04, 122.9)	(20.0, 36.30)	63.33	16.95	0.835	47.27	5.75E-03
0.005/L	316/43	10.48	(−66.64, −6.64, 122.3)	(20.0, 37.17)	59.33	16.32	0.911	55.44	7.51E-03
0.005/L	319/46	11.78	(−66.32, −6.32, 122.6)	(20.0, 38.71)	52.18	16.65	1.050	59.53	4.88E-03
0.005/L	322/49	9.18	(−66.39, −6.39, 122.5)	(20.0, 38.91)	51.27	16.58	0.962	50.04	7.03E-03

The intrinsic broadening brd, the CSA tensor components, the isotropic shift σ^{iso}, and the inhomogeneous broadening $\Delta\sigma^{aniso}$ are given in units of ppm. The curvature of the harmonic potential well V_0 in K. The CSA-orientation of the axis of the rapid rotation is given by the spherical polar angles (α, β) in the principal CSA-tensor frame and by the angle ϑ_{DR} with respect to the director. All the simulations were performed with angle ϑ_{LD} 90 degrees. (See reference [9] for detailed explanation of the parameters).

[a] Confidence of the least square fitting/G for Gauss and L for Lorentz lineshape (see text). The variance of the parameters in the final SIMPLEX was approximately equal to the given confidence value.

(c) The larger homogeneous broadening in the Glu sample indicated slower local motions of the phospholipid molecules [23]. The kind and mode of such motions cannot be specified by the present model. They can be: libration of the neighbouring protons, wobbling of the rotation axis, and lateral translation within one half of the bilayer lamellar formations [21,24].

In the following a detailed evaluation of the temperature variation of the broadline P-31-NMR-simulation parameters in connection to the properties of the bilayers and the effects of the inclusion will be attempted. The background of the simulations is given in our previous work [9].

3.2.3. Motional dynamics

By plotting the temperature dependence of the P-31-simulation parameters, motional dynamics information was gained. Most informative were shown to be the temperature profiles of the Homogeneous Broadening brd, (Fig. 7a) the Inhomogeneous Broadening $\Delta\sigma$ (Fig. 7b), and the Collective Tilt angle ϑ_{DR} (Fig. 7c).

In all three samples, i.e. both the unloaded and loaded DPPC/water bilayers with the dipeptide or Glu, the homogeneous broadening brd decreased monotonically with temperature, see Fig. 7a. The parameter *brd* is the intrinsic broadening imposed on the spin packets which were superimposed to form the inhomogeneous line. The high temperature spectra were simulated using Lorentzian lineshapes while below the pretransition temperature 35.3 °C the simulations necessitated Gaussian spin-packet lineshape (Table 3).

The tendency of decreasing *brd* with the temperature is due to the *increased mobility* of the *individual lipid molecules*, and was also reflected in an increased overall Cross-Polarization parameter *eNOE* (see Table 3). These tendencies are well understood within the Redfield relaxation theory [21]. According to the profile in Fig. 7a and within experimental error the *mobility* of the phospholipid molecules in the unloaded bilayers and the β-Ala-Tyr loaded bilayers were very similar. On the contrary, the phospholipids in the Glu loaded bilayers showed much less mobility, which in addition increased slower than in the other two samples. The above homogeneous broadening profiles showed none to very weak correlation to the phase transitions of the samples.

The residual anisotropy (inhomogeneous broadening) parameter $\Delta\sigma$ profiles in Fig. 7b, however showed certain correlation to the phase of the bilayer. The slope of the residual anisotropy profile, in particular for Glu, changed rather abruptly about the pretransition temperature, but the temperature resolution of the profiles in the present study did not allow the determination of the phase-transition temperature.

Furthermore this profile showed a relatively small sample-dependent variation, mainly in the ripple phase, just after the pretransition. The residual broadening decreased with temperature for all three samples indicating less restricted motion as the fluidity of the bilayer increased.

Finally, the Collective Tilt profiles in Fig. 7c displayed both significant variation among the three samples and also relatively strong correlation to the phase of the matter. The Glu loaded sample of the DPPC/water bilayers behaved very distinctly displaying maximal tilt angle ϑ_{DR}, which for all temperatures lay always little over 45 degrees.

The tilt of the β-Ala-Tyr loaded sample on the contrary was the smallest and had a close value to the one obtained for DPPC

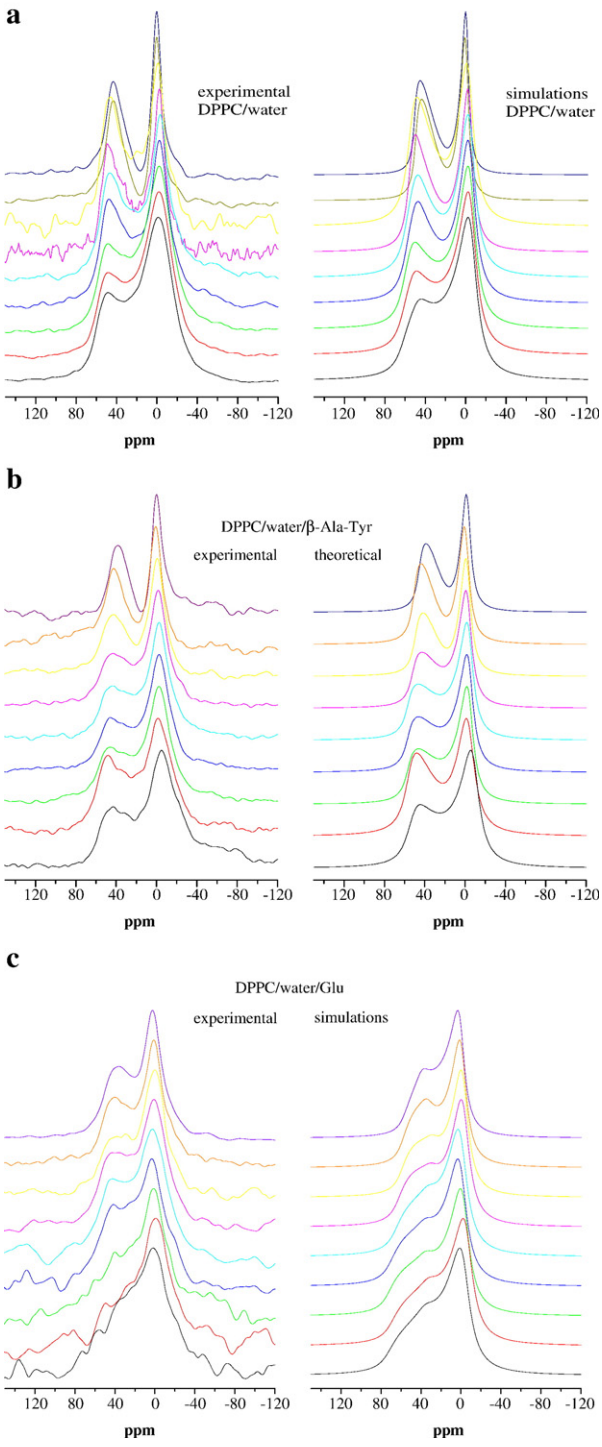

Fig. 6. Experimental and theoretical temperature-dependent lineshapes of static CP-^{31}P powders of: (a) pure DPPC/water multibilayers; (b) DPPC/water multibilayers containing (x=0.20) β-Ala-Tyr inclusion; (c) DPPC/water multibilayers containing (x=0.20) Glu inclusion. The temperatures of the lower to higher curves in each panel are: 25, 30, 33, 36, 38, 40, 43, 46, 49 °C.

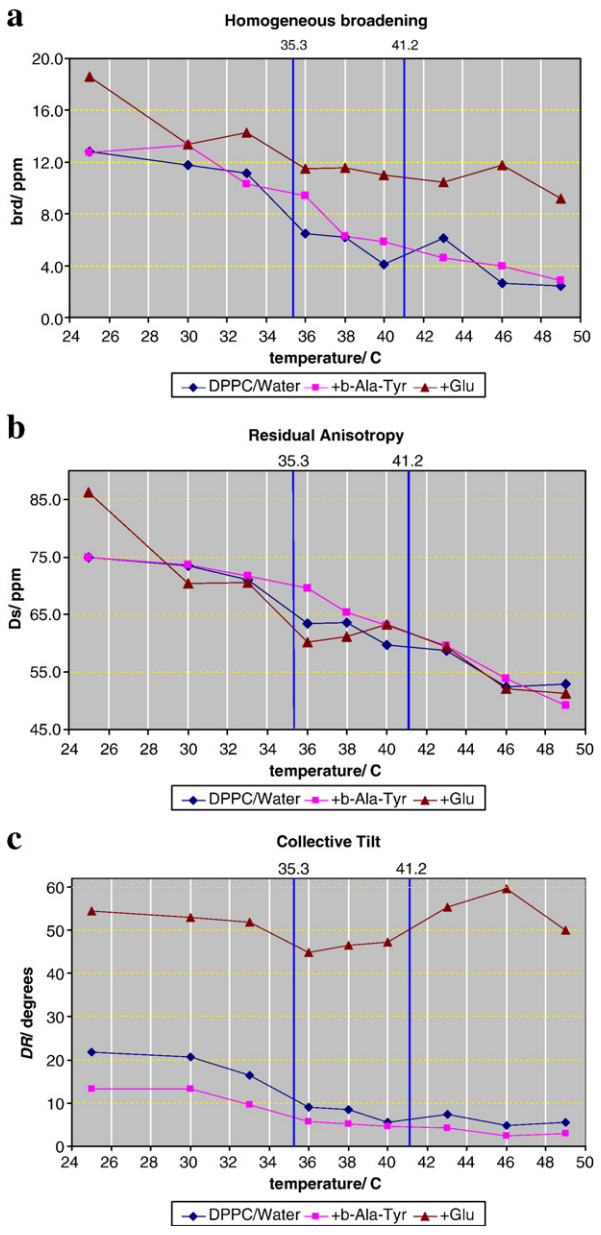

Fig. 7. Temperature profiles of the CP P-31 NMR broadline-simulations' parameters in the temperature interval 25 to 49 °C for: pure DPPC/water multibilayers; DPPC/water multibilayers containing (x=0.20) β-Ala-Tyr inclusion; DPPC/water multibilayers containing (x=0.20) Glu inclusion. The vertical lines correspond to the phase transition temperatures 35.3 and 41.2 °C. (a) Homogeneous broadening (b) Residual anisotropy (c) Collective tilt.

bilayers alone. This indicated a minor effect of the dipeptide inclusion in the lipid bilayers. In fact, the ordering in the magnitudes of the collective tilt profiles, as in Fig. 7c, indicated that the dipeptide destabilized the bilayer worsening the packing of the alkyl chains in the bilayer while the Glu increased the bilayer order. This is probably due to the topologies and the strength of the β-Ala-Tyr and Glu binding forces with the lipid molecules in the bilayers. As the Glu is attached in the headgroup it forced the lipids to a greater tilt [17] which improved the packing of the alkyl chains, while the dipeptide, being located in the higher hydrophobic zone of the bilayers decreased the order.

3.2.4. Raman spectroscopy

Raman spectra of the three preparations were obtained, namely, the unloaded DPPC bilayers, the bilayers with molar ratio β-Ala-Tyr/DPPC (x=0.20) and with Glu/DPPC (x=0.20). Experiments were performed at three temperatures that cover the stages of the lipid mesophase transitions (gel, ripple, liquid crystalline).

The C–C stretching modes in region 1050–1150 cm^{-1} reflect the intramolecular conformational changes within the hydrocarbon chain zone of the lipid matrix. In particular, the C–C peaks at 1090 and 1130 cm^{-1} are assigned to the stretching modes of the gauche and trans chain conformers, respectively, providing a way of estimation of the intrachain disorder [25,26]. The temperature profiles of the peak height intensity ratio I_{1090}/I_{1130} drawn in Fig. 8a permitted a direct comparison of the disorder/order characteristics between bilayers preparations with or without drug.

Thus, from Fig. 8a was concluded that the disorder is greatest for the dipeptide loaded DPPC/water bilayer during the entire experimental temperature range while the most ordered sample was the one loaded with Glu.

The methylene C–H stretching-mode in region 2800–3100 cm^{-1} provides the most intense bands in the Raman spectrum of lipid samples and has been commonly used to monitor changes in the lateral-packing properties and mobility of the lipid chain in both gel and liquid crystalline unilamellar and multi-lamellar bilayer systems [27]. In the spectrum of the gel state the methylene $>CH_2$ symmetric and asymmetric stretching modes appear as intense, partially overlapping peaks at 2847 and 2883 cm^{-1}, respectively. In particular, the 2850/2880 intensity index reflects primarily the interchain packing behaviour of the bilayers, while the intensity ratios of the complex Fermi resonance feature at 2935 cm^{-1} and the methylene asymmetric stretching modes at 2935–2880 cm^{-1} contain information reflecting both the inter- and intrachain disorder/order characteristics [28]. Thus, despite the fact that the C–H stretching mode region consists of many superimposed vibrational transitions, the peak height intensity ratios described above provide a sensitive probe combining intramolecular (conformational) chain disorder together with intermolecular chain–chain packing disorder [29].

The vibration spectrum of the Glu contained sharp peaks which overlapped significantly with the spectrum of the DPPC bilayers. Thus, the sharp peak at 2935 cm^{-1} of the Glu/DPPC/water sample in Fig. 9 was assigned to the Glu and not to DPPC. Since the C–H stretching region was dominated by the sharper Glu spectra it was not possible to obtain undisturbed the intensity ratio 2935/2880 cm^{-1} for DPPC/Glu bilayers.

The temperature profiles for the remaining two samples are shown in Fig. 8b indicating *greater disorder* for the sample loaded with the dipeptide β-Ala-Tyr compared to the unloaded DPPC/water bilayers.

Finally, the temperature profiles of the Raman intensity peak–height ratio (I_{2850}/I_{2880}) are shown in Fig. 8c indicating that in the three samples, the disorder was increasing in the following order: DPPC/Glu, DPPC alone, DPPC/β-Ala-Tyr. This result was identical to the one obtained by the temperature

profiles of the homogeneous broadening of the P-31 broadlines in Fig. 7c and can be summarized as following: The addition of β-Ala-Tyr or Glu in DPPC/water bilayers to 0.20 molar ratio inclusion (β-Ala-Tyr or Glu)/DPPC is affecting the packing of the bilayers in opposite ways. The dipeptide destabilized slightly the bilayers while the Glu increased the packing of the bilayers significantly.

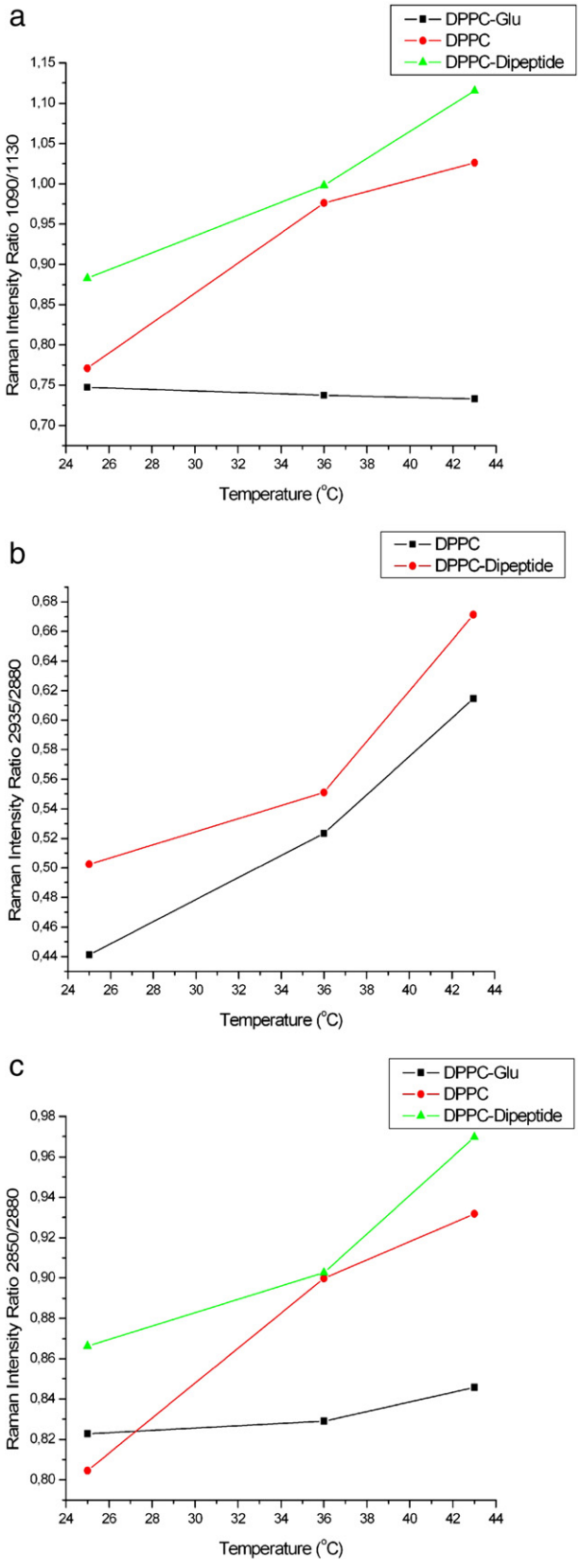

Fig. 8. (a) Temperature profiles of peak-height intensity ratios I_{1090}/I_{1130} (disorder/order) in the Raman spectra of unloaded DPPC/water bilayers and two samples of loaded DPPC/water bilayers with β-Ala-Tyr and Glu, both at a molar ratio inclusion/DPPC $x=0.2$. (b) The Raman intensity disorder/order ratio 2935/2880 cm^{-1} for the pure DPPC/water bilayers sample and the dipeptide loaded bilayers. (c) Temperature profiles of peak–height intensity disorder/order ratios I_{2850}/I_{2880} in the Raman spectra of unloaded DPPC/water bilayers and two samples of loaded DPPC/water bilayers with β-Ala-Tyr and Glu, both at a molar ratio inclusion/DPPC $x=0.2$.

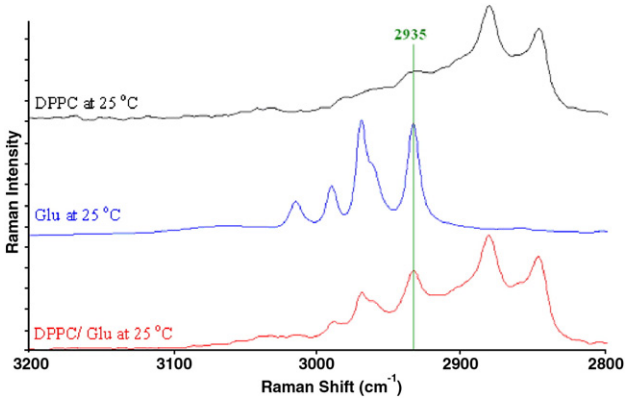

Fig. 9. Inspection of the C–H stretching bands for DPPC/water bilayers, Glu and DPPC/water/Glu samples.

It is worthwhile to mention that there is a direct evidence for the strong interaction of the Glu with the choline in the headgroup from the Raman spectra of the DPPC/water/Glu bilayers. The shifts of the headgroup choline peak with the temperature change are shown in Fig. 10 after addition of dipeptide or Glu in the bilayer. The smaller the shift the greater the stabilization of the choline peak against the temperature variation. Thus, the much smaller shift of 2.1 cm^{-1} of the dipeptide loaded sample (Fig. 10a) compared to the shift of 7.1 cm^{-1} of the Glu loaded sample (Fig. 10b) indicates that the dipeptide resides in longer distance from choline than Glu, most probably inside the higher aliphatic zone of the bilayer close to the glycerol backbone.

4. Conclusions

The DSC data showed that Glu perturbed more the DPPC/water bilayers than the dipeptide β-Ala-Tyr, as depicted by the changes of the diagnostic DSC parameters T_m, $T_{m;1/2}$ and ΔH.

High resolution solid-state MAS data ^{13}C-NMR indicated also that Glu disturbs more than the dipeptide the lineshapes attributed to the phospholipids of the DPPC bilayers. In particular, Glu caused a significant increase of the width of the lineshape indicating the existence of inhomogeneity or domains in the lipid bilayers in corroboration with the DSC and the Raman experiments. The changes in the ^{13}C-NMR lineshapes of the peaks due to the presence of β-Ala-Tyr dipeptide were not as pronounced. These results were also in harmony with DSC data which showed that β-Ala-Tyr did not affect significantly

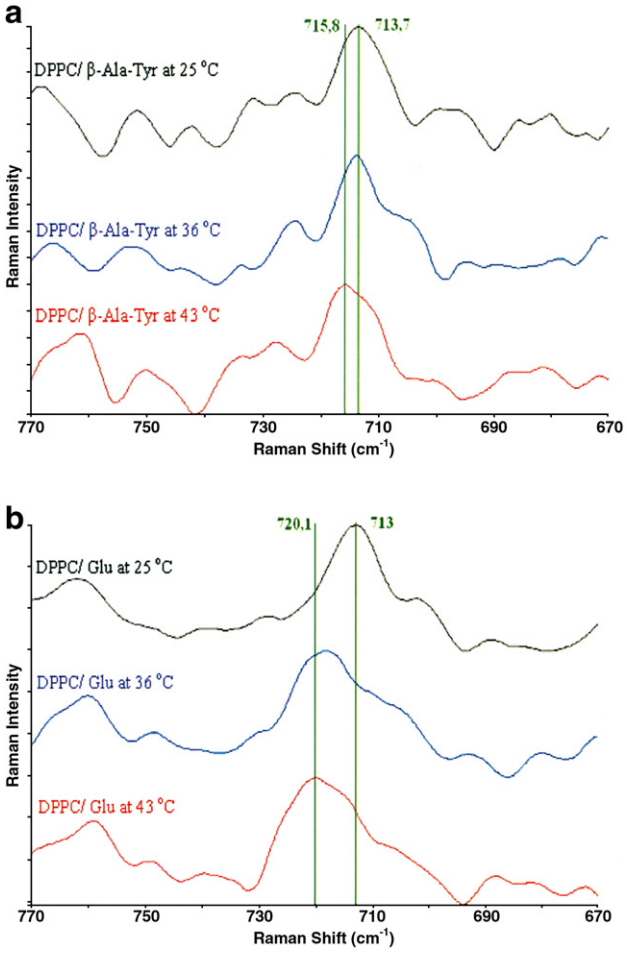

Fig. 10. (a) The peak of the headgroup choline for three experimental temperatures, 25 °C, 36 °C and 43 °C of the DPPC/water bilayers with the inclusion of dipeptide β-Ala-Tyr. (b) The peak of the headgroup choline for three experimental temperatures, 25 °C, 36 °C and 43 °C of the DPPC/water bilayers with the inclusion of dipeptide Glu.

the thermal profile of DPPC bilayers loaded with the dipeptide. The T_1 values of the ^{13}C showed that the presence of β-Ala-Tyr caused increase in the flexibility of the lipid head-group and the alkyl chains. Glu on the other hand exerted a different and stronger effect on the alkyl chains than β-Ala-Tyr. Results from Raman Spectroscopy are complementary indicating a strong effect of increasing order for the bilayers containing Glu and an opposite and less perturbing effect by the bilayers containing β-Ala-Tyr.

The broadline P-31 NMR spectra of DPPC/water/β-Ala-Tyr were very similar with those of unloaded DPPC/water bilayers in contrast to the P-31 spectra of the DPPC/water/Glu bilayers, which possessed some distinct characteristics. Thus, the Glu molecules perturbed more the CP ^{31}P-NMR broadlines of DPPC/water bilayers than β-Ala-Tyr. The most possible attachment of Glu is the region of the choline fragment at the head-group of the phospholipid molecule in the lipid/water interface. The dipeptide was on the other hand localized not as close to the phosphate as the Glu but was instead located in the edge to the hydrophobic segment of the bilayers. In particular the aromatic segment was anchoring in the hydrophobic zone of the acyl chains [30]. Furthermore, the orientation of the axis of the (uniaxial) rotation was shown to deviate significantly from the normal to the surface of the bilayer lamellae in the Glu sample. Thus, Glu interacts directly with the phosphate and probably forces a collective tilt of the lipid chains with respect to the lamellar normal [17]. This is equivalent to improved packing of the lipid molecules in the bilayers in agreement with DSC, and Raman spectroscopy data.

In conclusion, the combination of the three biophysical methods, DSC, Raman and NMR revealed the different effects of the two molecules on the lipids at the molecular level. Glu was strongly associated in the vicinity of the phosphate as clearly DSC, Raman and ^{31}P stationary NMR data demonstrated. Such an association is lacking for the dipeptide β-Ala-Tyr which probably resided at the upper region of the alkyl chains in the hydrophobic layer. This topology of Tyr in lipid bilayers was actually anticipated by Killian and co-workers, see de Planque et al. [30]. That work revealed the interfacial property of aromatic Trp (Tryptophan) residues of trans-membrane peptides in lipid bilayers to anchor in the polar/apolar "interface" of the bilayers, due to the amphoteric properties of the indole ring terminal of Trp.

The lipophilic profile of β-Ala-Tyr may explain the mild thermal effects that was caused on the thermal profile of DPPC bilayers and the similarity of ^{13}C high resolution spectra (and ^{31}P solid state) of DPPC/water bilayers containing β-Ala-Tyr and unloaded DPPC/water bilayers.

Acknowledgement

This research activity was financed by the General Secretariat for Research and Technology of Greece through ENTER 04ER52.

References

[1] S.-J. Chiou, S. Kotanen, A. Cerstianes, D. Daloze, J. Pasteels, A. Lesage, W. Drifhout, P. Verhaer, L. Dillen, M. Clayes, H. De Meulemeester, B. Nuttin, A. De Loof, L. Schoofs, Purification of toxic compounds from larvae of the gray fleshfly: the identification of paralysins, Biochem. Biophys. Res. Commun. 246 (1998) 457–462.
[2] S.-J. Chiou, A. Cerstiaens, S.P. Kotanen, A. De Loof, L. Schoofs, Insect larvae contain substances toxic to adults: the discovery of paralysins, J. Insect Physiol. 44 (1998) 405–411.
[3] A.M. Craig, Activity and synaptic receptor targeting: the long view, Neuron 21 (1998) 459–462.
[4] I. Song, S. Kamboj, J. Xia, H. Dong, D. Liao, R.L. Huganir, Interaction of N-ethylmaleimide-sensitive factor with AMPA receptors, Neuron 21 (1998) 393–400.
[5] R.J. O´Brien, L.-F. Lau, R.L. Huganir, Molecular mechanisms of glutamate receptor clustering at excitatory synapses, Cur. Opt. Neurobiol. 8 (1998) 364–369.
[6] M. Salzet, Neuropeptide-derived antimicrobial peptides from invertebrates for biomedical applications, Curr. Med. Chem. 12 (2005) 2663–2681.
[7] T. Mavromoustakos, E. Theodoropoulou, De-Ping Yang, The use of high-resolution solid-state NMR spectroscopy and differential scanning calorimetry to study interactions of anaesthetic steroids with membrane, Biochim. Biophys. Acta 1328 (1997) 65–73.
[8] F.A.L. Anet, D.J. O'Leary, The shielding tensor. Part I: understanding its symmetry properties, Conc. Magn. Res. 3 (1991) 193–214.
[9] N.P. Benetis, I. Kyrikou, M. Zervou, T. Mavromoustakos, Static ^{31}P CP

NMR multilamellar bilayer broadlines in the absence and presence of the bioactive dipeptide β-Ala-Tyr or Glu, Chem. Phys. 314 (1–3) (2005) 57–72.
[10] A. Pines, M.G. Gibby, J.S. Waugh, Proton-enhanced NMR of dilute spins in solids, J. Chem. Phys. 59 (2) (1973) 569–590.
[11] P.L. Yeagle, Phosphorous NMR of membranes, Biol. Magn. Reson. 9 (1) (1990) 153.
[12] J. Frye, A.D. Albert, B.S. Selinsky, P.L. Yeagle, Cross polarization P-31 nuclear magnetic resonance of phospholipids, J. Biophys. 48 (1985) 547–552.
[13] R.F. Cambell, E. Meirovitch, J.H. Freed, Slow-motional NMR line shapes for very anisotropic rotational diffusion. Phosphorous-31 NMR of phospholipids, J. Phys. Chem. 83 (4) (1979) 525–533.
[14] Wen-guey Wu, Lang-Ming Chi, Comparisons of lipid dynamics and packing in fully interdigitated monoarachidoylphosphatidylcholine and non-interdigitated dipalmitoyl-phosphatidyl-choline bilayers: cross polarization/magic angle spinning ^{13}C-NMR studies, Biochim. Biophys. Acta 1026 (1990) 225–235.
[15] I. Kyrikou, S.G. Grdadolnik, M. Tatari, C. Poulos, T. Mavromoustakos, Structural elucidation and conformational properties of the toxin paralysin β-Ala-Tyr, J. Pharm. Biomed. Anal. 31 (2003) 713–721.
[16] T. Mavromoustakos, P. Zoumpoulakis, I. Kyrikou, A. Zoga, E. Siapi, M. Zervou, I. Daliani, D. Dimitriou, A. Pitsas, C. Kamoutsis, P. Laggner, Efforts to understand the molecular basis of hypertension trough drug: membrane interactions, Curr. Top. Med. Chem. 2004 (4) (2003) 385–401.
[17] M.D. Houslay, K.K. Stanley, Dynamics of Biological Membranes, John Wiley and Sons, New York, 1982.
[18] T. Mavromoustakos, E. Theodoropoulou, A combined use of ^{13}C-cross polarization/magic angle spinning, ^{13}C-magic angle spinning and ^{31}P-nuclear magnetic resonance spectroscopy with differential scanning calorimetry to study cannabinoid–membrane interactions, Chem. Phys. Lipids 92 (1998) 37.
[19] P. Zoumpoulakis, I. Daliani, M. Zervou, I. Kyrikou, E. Siapi, G. Lamprinidis, E. Mikros, T. Mavromoustakos, Losartan's molecular basis of interaction with membranes and AT_1 receptor, Chem. Phys. Lipids 125 (2003) 13–25.
[20] R.R. Ernst, G. Bodenhausen, A. Wokaun, Principles of Magnetic Resonance in One and Two Dimensions, Clarendon Press, Oxford, 1991.
[21] N.P. Benetis, Dynamical Effects in CW and Pulsed EPR, in: A. Lund, M. Shiotani (Eds.), EPR of Free Radicals Solids. Part I Trends in methods, Kluwer, 2003 (Chapt. 3).
[22] P.L. Yeagle, Phosphorous NMR of membranes, Biol. Magn. Reson. 9 (1) (1990) 153.
[23] B.A. Cornell, J.B. Davenport, F. Separovic, Low-frequency motion in membranes. The effect of cholesterol and proteins, Biochim. Biophys. Acta 689 (2) (1982) 337–345.
[24] F. Separovic, B. Cornell, R. Pace, Orientation dependence of NMR relaxation time, T1ρ, in lipid bilayers, Chem. Phys. Lipids 107 (2000) 159–167.
[25] J.R. Silvius, M. Lyons, P.L. Yeagle, T.J. O'Leary, Thermotropic properties of bilayers containing branched-chain phospholipids, Calorimetric, Raman and ^{31}P NMR studies, Biochem. 24 (1985) 5388–5395.
[26] T. O'Leary, P.D. Ross, I.W. Levin, Effects of anaesthetic and nonanaesthetic steroids on dipalmitoylphosphatidylcholine liposome: a Calorimetric and Raman spectroscopic investigation, Biochemistry 23 (1984) 4636–4641.
[27] Ch-h. Huang, J.R. Lapides, I.W. Levin, Phase-transition behaviour of saturated, symmetric chain phospholipid bilayers dispersions determined by Raman spectroscopy: correlation between spectral and thermodynamic parameters, J. Am. Chem. Soc. 104 (1982) 5926–5930.
[28] I.W. Levin, E.N. Lewis, Fourier transform Raman spectroscopy of biological materials, Anal. Chem. 62 (21) (1990) 1101A–1111A.
[29] R.G. Snyder, J.R. Scherer, B.P. Gaber, Effects of chain packing and chain mobility on the Raman spectra of biomembranes, Biochim. Biophys. Acta 601 (1980) 47–53.
[30] M.R.R. De Planque, B.B. Bonev, J.A.A. Demmers, D.V. Greathouse, R.E. Koeppe II, F. Separovic, A. Watts, J.A. Killian, Interfacial anchor properties of tryptophan residues in transmembrane peptides can dominate over hydrophobic matching effects in peptide–lipid interactions, Biochemistry 42 (2003) 5341–5348.